powders

MDPI

Article

A Carbon-Free Way for Obtaining Nanoscale Silicon

Nikolay Lyakhov [1,2,*], Tatiana Grigoreva [1,*], Tatiana Talako [3], Tatyana Udalova [1,4], Sergey Vosmerikov [1] and Evgeniya Devyatkina [1]

[1] Institute of Solid State Chemistry and Mechanochemistry of the Siberian Branch of the Russian Academy of Sciences, 18 Kutateladze Street, 630128 Novosibirsk, Russia; udalova@solid.nsc.ru (T.U.); vosmerikov@solid.nsc.ru (S.V.); devyatkina@solid.nsc.ru (E.D.)
[2] Department of Chemical Materials Science, Faculty of Natural Sciences, Novosibirsk State University, 1 Pirogov Street, 630090 Novosibirsk, Russia
[3] Department of Physical and Technical Sciences of National Academy of Sciences of Belarus, 66 Nezavisimosti Avenue, 220072 Minsk, Belarus; talako@presidium.bas-net.by
[4] Department of Chemistry and Chemical Technology, Faculty of Mechanics and Technology, Novosibirsk State Technical University, 20 K. Marks Avenue, 630073 Novosibirsk, Russia
* Correspondence: lyakhov@solid.nsc.ru (N.L.); grig@solid.nsc.ru (T.G.); Tel.: +7-383-2332410 (ext. 1111) (N.L.); +7-383-2332410 (ext. 1546) (T.G.)

Abstract: The nanosized silicon powder has been produced by reduction of silica with magnesium in an argon medium using both the mechanically activated self-propagating high-temperature synthesis and the direct mechanochemical synthesis and has been investigated by X-ray phase analysis, Infrared spectroscopy, electron scanning microscopy, and energy dispersive X-ray spectroscopy. The optimal Mg:SiO_2 ratio has been found to provide the minimum content of contaminant impurities of magnesium silicide and silicate in mechanically activated self-propagating high-temperature synthesis. For the first time, direct mechanochemical synthesis of Si via reduction of silica with magnesium has been implemented. Optimal component ratio and mechanical activation parameters have been determined, yielding Si/MgO composites without impurity phases (magnesium silicide and silicate). A purification procedure has been proposed for separating silicon obtained from magnesium oxide and other impurity phases. The ratio of initial components has been determined, at which purified silicon has the least amount of impurities. The particle size of silicon powder obtained was 50–80 nm for the mechanically activated self-propagating high-temperature synthesis, and 30–50 nm for the direct mechanochemical synthesis.

Keywords: mechanical activation; self-propagating high-temperature synthesis; mechanochemical synthesis; silica; magnesium; silicon; reduction reactions

Citation: Lyakhov, N.; Grigoreva, T.; Talako, T.; Udalova, T.; Vosmerikov, S.; Devyatkina, E. A Carbon-Free Way for Obtaining Nanoscale Silicon. *Powders* **2022**, *1*, 18–32. https://doi.org/10.3390/powders1010003

Academic Editor: Khaled Morsi

Received: 30 December 2021
Accepted: 10 February 2022
Published: 17 February 2022

1. Introduction

Nanostructured silicon is a promising material for lithium-ion batteries [1,2], photovoltaics systems [3,4], photocatalysis [5], nanoenergetics materials [6], and thermoelectrics [7,8]. Metallurgical-grade silicon is industrially produced by carbothermal reduction of silica [9]. However, this process cannot fabricate nanostructured material as the temperature of carbothermic reduction (over 1900 °C) is higher than the melting point of silicon (1414 °C). In addition, this process is multistage, energy consuming, and rather dangerous ecologically. Therefore, the development of alternative time- and energy-saving technologies that also reduce the cost of the final product is an extremely desirable task.

One of the most common carbon-free methods for obtaining silicon for most highly exothermic systems is self-propagating high-temperature synthesis (SHS) [10–12]. However, in systems where the combustion temperatures are significantly higher than the melting temperatures of the reactants (first of all, magnesium- and aluminothermic processes), the preparation of powder nanosized products is a serious problem. Usually, a decrease in

the combustion temperature in SHS is achieved by diluting the reaction mixture with the reaction products [13–16].

In recent years, there has been a growing interest in mechanical activation/high-energy ball-milling as one of the options to reduce combustion temperature and to obtain nanosized or nanostructured materials [17–20]. However, in this case, the process becomes two- (MA + SHS = MA SHS) or three-stage (MA + SHS + MA = MA SHS MA) [21–23]. For a number of oxides, the possibility of direct mechanochemical reduction by active metals was shown [24]. For example, magnesium was used for reduction of copper [25,26], vanadium [27,28], tungsten [29], and iron [30] oxides.

It was shown that for some high-energy systems, reactions can proceed in SHS or mechanically activated self-propagating high-temperature synthesis (MA SHS) mode but cannot be implemented purely mechanochemically (in an activator). For example, the reduction of SiO_2 with aluminum was carried out by the MA SHS process [27,31], but it was not possible to reduce SiO_2 mechanochemically to silicon under any MA regimes [31].

The purpose of this work was to study the possibility of direct mechanochemical reduction of silica with magnesium to obtain nanosized silicon powder, as well as to compare the structural and morphological characteristics of products obtained by different methods using mechanochemistry.

2. Materials and Methods

The following reagents were used in the work: nanoscale pyrogenic SiO_2 (aerosil) with a particle size of <10 nm (99.8% pure) from SILIKA LLC (Dolgoprudny, Moscow region, Russia); magnesium shavings MGS-99 (99.7% pure) from Ruskhim.ru LLC (Moscow, Russia); hydrochloric acid, "highly pure grade", acetic acid, "chemically pure grade", and hydrofluoric acid 70%, "highly pure grade" from CHIMEX LTD (Moscow, Russia).

Mixtures of silica and metallic magnesium with different component ratios were processed in a high-energy planetary ball mill AGO-2 with water cooling (drum volume 250 cm^3, steel ball diameter 5 mm, ball loading 200 g, sample weight 10 g, and the rotation speed of drums around the common axis ~1000 rpm or ~600 rpm, which corresponds to a centrifugal acceleration 60 *g* and 20 *g* respectively).

An upper-drive mixer RZR 1 (HEIDOLPH, Schwabach, Germany) with rotation speed 1000 rpm was used during the acid treatment of MA SHS samples. The separation of silicon from impurities for the products of both MA SHS and direct mechanochemical reduction was carried out by three-stage acid treatment [32]. The sample was sequentially treated with a 2 M solution of HCl; with a mixture of 2 M HCl and 20–25% CH_3COOH; with a mixture of 5% HF and 20–25% CH_3COOH. Acid treatment conditions were τ = 1 h, T = 70–80 °C. After each acid treatment stage, the suspension was centrifuged and the precipitate was washed with distilled water and extracted from the aqueous phase by decantation.

Infrared (IR) spectra were registered on a Tensor-27 spectrometer (Bruker Optik GmbH, Ettlingen, Germany) in the wavenumber range of 4000–400 cm^{-1}. The samples for the study were compacted with calcinated potassium bromide [33].

X-ray investigations were carried out on a D8 Advance diffractometer (Bruker AXS GmbH, Karlsruhe, Germany, CuK_α-radiation, λ = 1.5418 Å). Phase composition and crystal structure of the samples were determined by X-ray diffraction data using the database of the International Centre for Diffraction Data (ICDD) PDF4 [34].

Morphology of obtained samples was studied using scanning electron microscopes (SEM): Hitachi TM 1000 (Tokyo, Japan) (at accelerating voltage of 15 kV) equipped with a TM1000 EDS detector to determine the chemical composition of the sample and high-resolution SEM by MIRA\TESCAN with an energy-dispersive X-ray (EDX) attachment by OXFORD INSTRUMENTS (Abingdon, Oxfordshire, UK).

The content of impurity elements in the obtained silicon powders was studied using an atomic emission spectrometer with inductively coupled plasma AKTIVA M («HORIBA Jobin Yvon S.A.S», Longjumeau, France) (elements from F to U, detection limit from 0.1 ppb).

3. Results

3.1. Study of the MA SHS Reduction of Silica by Magnesium

Mechanochemical reactions of silica reduction with magnesium were carried out under different modes of mechanical activation and with different component ratios.

According to IR spectroscopy data, when processed for 40 s in a high-energy ball mill with a maximum load of 60 *g*, the product mainly contains magnesium silicate Mg_2SiO_4 (Figure 1, curve 2).

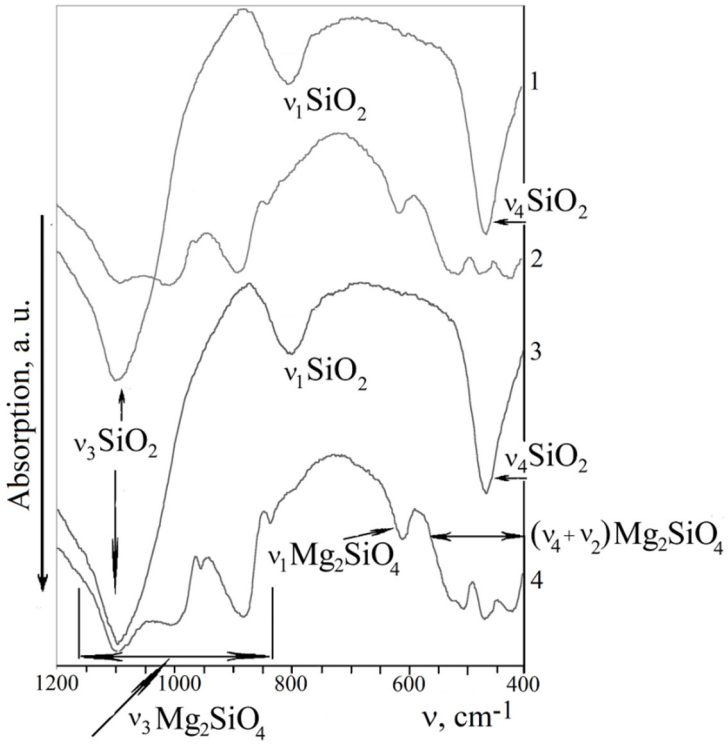

Figure 1. IR spectra of mixtures Mg:SiO_2 of stoichiometric composition (2:1) after mechanical activation: initial mixture (1); centrifugal acceleration 60 *g*, MA time 1 min (2); centrifugal acceleration 20 *g*, MA time 40 s (3); centrifugal acceleration 20 *g*, MA time 4 min (4).

When the rotation speed decreases to 600 rpm and the activation duration is less than 2 min, Mg_2SiO_4 is not formed and SiO_2 bands are kept in the spectrum. Under such treatment conditions, formation of silicates begins after 4 min of activation.

The mechanical activation mode (duration 40 s at a load of 20 *g*) worked-off for the stoichiometric composition Mg/SiO_2 = 2:1 was applied for the preparation of Mg/SiO_2 precursors with other component ratios also used for further SHS processes:

1. Molar ratio of Mg:SiO_2 = 1.5:1;
2. Molar ratio of Mg:SiO_2 = 2:1, stoichiometry;
3. Molar ratio of Mg:SiO_2 = 2.5:1;
4. Molar ratio of Mg:SiO_2 = 3:1;
5. Molar ratio of Mg:SiO_2 = 4:1.

The X-ray diffraction (XRD) patterns of Mg/SiO_2 precursors with different component ratios (Figure 2) are consistent with the IR spectroscopy data.

X-ray phase analysis of the mechanochemically obtained precursors did not show any traces of phase transformations during mechanical activation at these durations. Only intensities of magnesium diffraction reflections change with MA (Figure 2), and SiO_2 used in this work is X-ray amorphous.

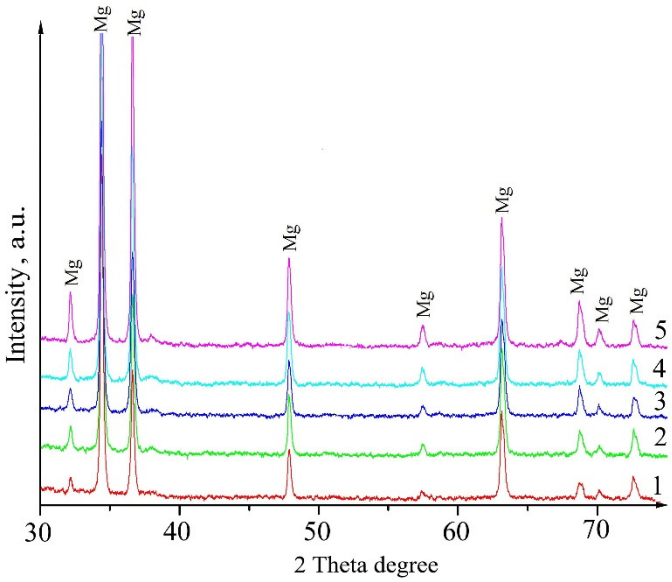

Figure 2. X-ray diffraction patterns of MA products of mixtures with different molar ratios of Mg:SiO_2, curves: 1.5:1 (1); 2:1 (2); 2.5:1 (3); 3:1 (4); 4:1 (5); the MA duration is 40 s, a load of 20 *g* (600 rpm).

The excessive magnesium content was added to speed up the heat removal during the SHS process, resulting in reduction of combustion temperature.

Investigation of the SHS process in mechanochemically obtained Mg/SiO_2 composites as the precursors showed that even a short–term MA (20–60 *g*) allows igniting the combustion in powder mixtures without preheating. For all compositions studied, a very rapid heat evolution takes place in the combustion front (due to the magnesiothermal reaction) (Figure 3).

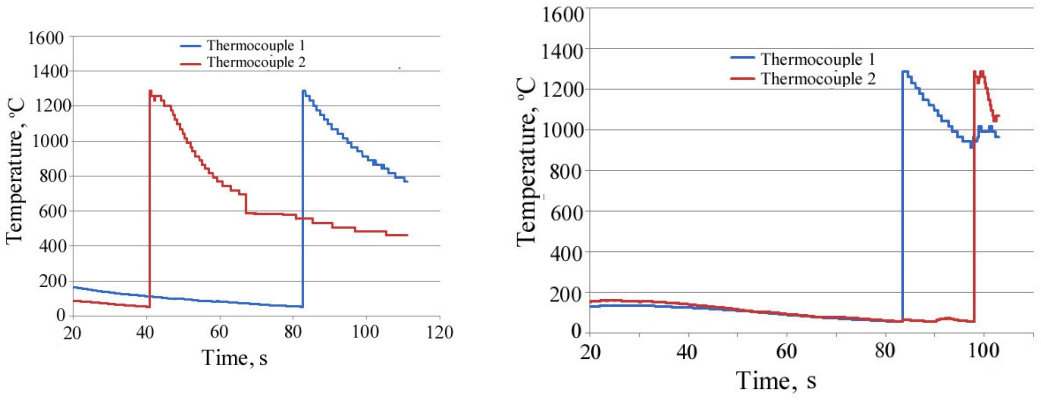

Figure 3. Combustion thermograms of the mechanocomposites Mg/SiO_2 = 2:1 vs. intensity and duration of activation: (**a**) 600 rpm, 60 s; (**b**) 1000 rpm, 20 s.

Figure 3 shows that an increase in the MA duration leads to a decrease in the ignition delay time t_d. Thus, after MA for 20 s (at 1000 rpm), the $t_d \approx 80$ s, while after 60 s MA (at 600 rpm), the initiation of the reaction is observed after ≈40 s. The maximum combustion temperature (T_C ~ 1283–1288 °C) is achieved for the stoichiometric composition (sample no. 2) (Figure 3). According to [35], the adiabatic temperature of the reaction 2Mg (s) + SiO_2 (s) → 2MgO (s) + Si for the stoichiometric composition (45% Mg) is 2123 K (1850 °C). At the same time, the calculation of the adiabatic temperature in the ISMAN-TERMO program, presented in [13], gives a temperature of 1900 °C (it decreases when diluents are used). In our case, for a stoichiometric composition, the maximum combustion

temperature is T_C ~ 1283–1288 °C, which is lower than the calculated adiabatic temperature given above. This is due to the complex and not yet fully disclosed mechanism of the influence of MA on the combustion parameters [22,36,37].

It is evident from Figure 3 that an increase in the MA duration results in the essential decrease in the ignition delay time t_d even for a lower intensive mode of MA. Thus, t_d is about 80 s for 20 s of MA at a load of 60 *g*, while the delay time of about 40 s is observed after MA for 1 min at a load of 20 *g*. Herewith, the propagation velocity of the combustion wave for a longer but less intensive MA mode is significantly lower (0.35 mm/s compared to 1.03 mm/s for a load of 60 *g* and 20 s of MA).

In a sample with a lack of magnesium (no. 1) T_C is slightly lower (~1100 °C). Combustion temperature in samples with excess magnesium content is about 1020–1050 °C.

Analysis of the phase composition of combustion products in the systems under investigation showed that at a molar ratio of Mg:SiO_2 from 1.5 to 4, the products of MA SHS, except Si and MgO, contain a small amount of Mg_2Si and Mg_2SiO_4.

Herewith, the duration of MA has a greater effect on the relative content of magnesium silicate than the mill power in the studied range of values (20–60 *g*), and the phase composition of the synthesis products is mainly dependent on the component ratio of the charge mixture (Figure 4).

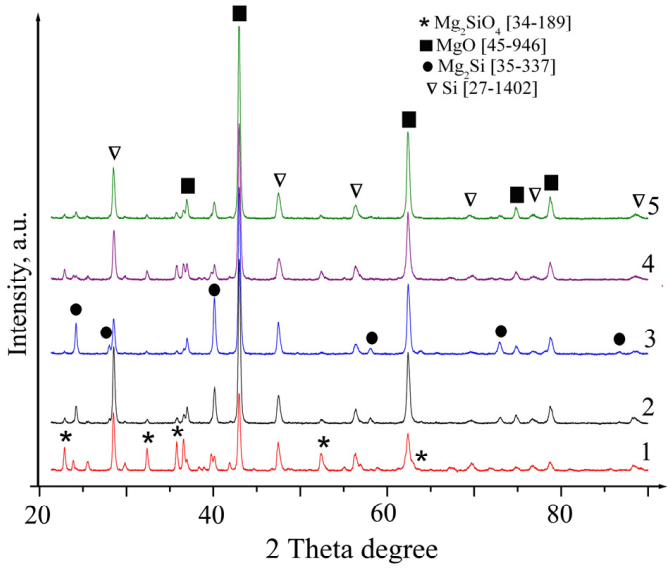

Figure 4. X-ray diffraction patterns of MA SHS products in a reaction mixture of various compositions Mg:SiO_2, curves: 1.5:1 (1); 2:1 (2); 2.5:1 (3); 3:1 (4); 4:1 (5). MA mode before SHS: MA time 40 s at a load of 20 *g* (600 rpm).

According to the XRD data, the main products of SHS are silicon and magnesium oxide. The formation of some amounts of silicate and magnesium silicide is also confirmed. The Mg_2Si content significantly increases with the excess of magnesium, and the greatest intensity of its reflexes is achieved at Mg/SiO_2 = 2.5:1 (Figure 4, curve 3). The strongest peak of Mg_2Si in curve 3 can be explained by the high rate of silicon formation at the presence of the excessive magnesium and rapid interaction of small particles of the reduced silicon with magnesium in the mechanically activated material (nanocomposite). With an increase in the magnesium excess, the relative silicon content and the rate of silicon formation, as well as contact surface between the reactants, decrease. Therefore, the formation of magnesium silicide is suppressed, which is observed in curves 4 and 5. The concentration of magnesium silicate is the lowest at the component ratio 2.5:1, i.e., the lowest intensity of Mg_2SiO_4 reflexes is identified in X-ray diffraction patterns of MA SHS products as compared with that of other Mg:SiO_2 ratios (Figure 4, curve 3). It should be noted that it is easier to perform chemical separation of silicon from silicide than from magnesium silicate.

Figure 5a–c show the microstructure and elemental mapping of the MA SHS product in a stoichiometric reaction mixture after MA at 60 *g* for 20 s. Rounded silicon particles ranging in size from 1 to 15 μm are clearly distinguished in the matrix of magnesium oxide. Relatively large regions containing all the elements of the composition (obviously Mg_2SiO_4) with the diffused boundaries of individual Si and MgO particles are revealed after MA at 20 *g* for 60 s (Figure 5d–f).

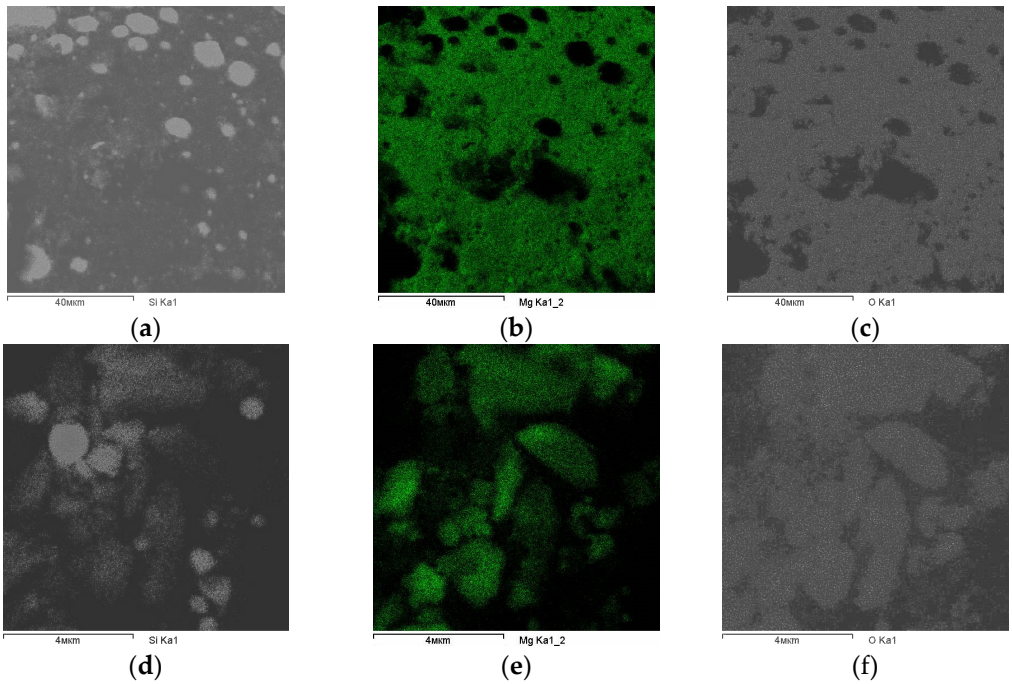

Figure 5. SEM-images of the cross-sections and the elemental mapping (Si, Mg, O) of MA SHS product (Mg/SiO_2 = 2:1) vs the MA mode. (**a**–**c**) 60 *g*, 20 s; (**d**–**f**) 20 *g*, 60 s; (**a**,**d**) Si; (**b**,**e**) Mg; (**c**,**f**) O.

The IR spectra of the MA SHS products indicate the formation of magnesium silicates of larger or smaller quantities in all mixtures investigated.

Based on the XRD results, a certain amount of silicates and magnesium silicide was identified in the products after leaching with hydrochloric acid. For a more complete removal of magnesium compounds, the second stage of treatment of the sample with a mixture of acetic and hydrochloric acids was carried out. The addition of acetic acid reduces the adsorption of metal cations on silicon powder.

The treatment of precipitations with a mixture of hydrofluoric and acetic acids was used at the final purification stage.

According to the X-ray phase analysis of silicon powders obtained from all the compositions, MgO, Mg_2Si, and Mg_2SiO_4 reflexes are not observed in the XRD patterns after three-stage purification (Figure 6).

EDX analysis of all the investigated silicon powders after purification did not reveal a noticeable presence of impurities (within the limits of detection errors).

Further studies of the impurity content in the as-obtained silicon powders were carried out using a certified atomic emission spectrometer with inductively coupled plasma "ACTIVA M" (France). The error of the method was 3–5% relative.

The data on the content of impurity elements in silicon powders after the three-stage acid treatment are presented in Table 1. As can be seen from Table 1, the purity of silicon strongly depends on the ratio of the initial components in the reaction mixture. In the powder obtained from the reaction mixture of stoichiometric composition, a certain amount of magnesium (1.1%) is retained after leaching. In the sample obtained at the ratio Mg/SiO_2 = 2.5:1, the magnesium content is at the level of other impurity elements. Obviously, this is due to the predominant formation of magnesium silicide and insignificant

content of Mg_2SiO_4 silicate in the synthesis product. Thus, the purity of the silicon powder obtained at the stoichiometric ratio of the components of the reaction mixture is 98.45%. The powder obtained at the ratio Mg/SiO_2 = 2.5:1 is much more pure (99.57%) with the same purification technology.

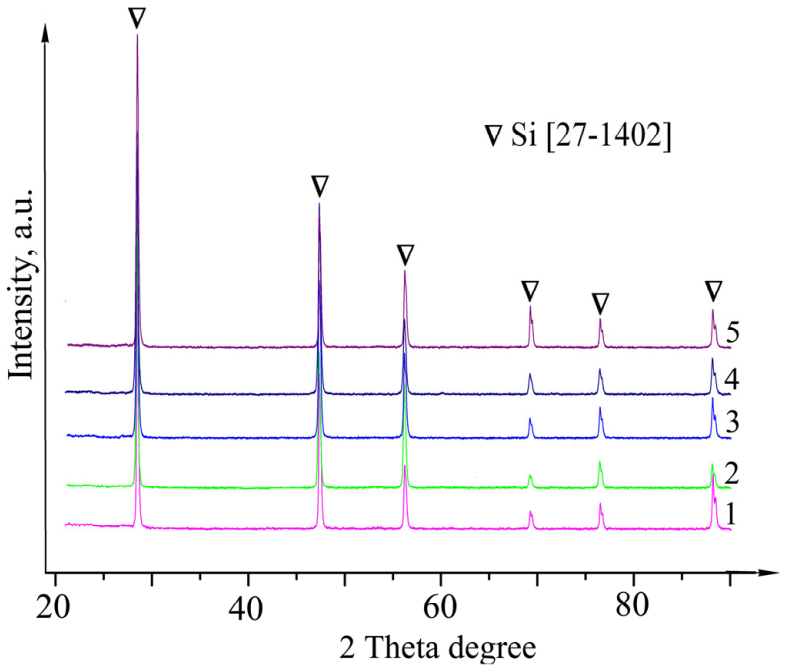

Figure 6. X-ray diffraction patterns of samples after three-stage acid treatment of products of MA SHS mixtures of compositions $Mg:SiO_2$, curves: 1.5:1 (1); 2:1 (2); 2.5:1 (3); 3:1 (4); 4:1 (5). The MA duration before the SHS is 40 s (20 *g*).

Table 1. The content of impurity elements in the obtained silicon powders after the three-stage acid treatment of the samples with different Mg/SiO_2 molar ratios.

Impurity	Molar Ratio = 2:1	Molar Ratio = 2.5:1
Al	0.02	0.02
Ca	0.08	0.07
Cd	0.03	0.01
Cr	0.02	0.02
Fe	0.05	0.03
K	0.2	0.14
Mg	1.1	0.08
Mn	less than 0.01	less than 0.01
Ni	0.03	0.04
Zn	less than 0.01	less than 0.01
Si	98.45	99.57

Preliminary studies of morphology of purified silicon samples by the SEM at the lower magnifications showed that the average size of the particle agglomerates is about 1–10 μm. SEM micrographs at the higher magnifications show that the agglomerated powders consist of smaller particles with a small size range (Figure 7).

The agglomerates of samples with molar ratio $Mg:SiO_2$ = 2:1 and 2.5:1 consist of nanodispersed particles with the particle size about 50–80 nm (Figure 8).

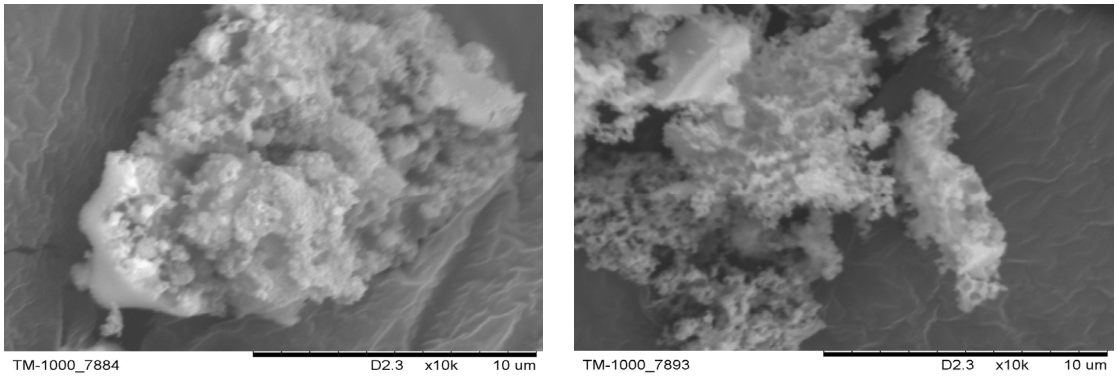

(**a**) (**b**)

Figure 7. SEM images of the purified silicon powders produced from the mixtures at ratio $Mg:SiO_2$ = 2:1 (**a**); 2.5:1 (**b**).

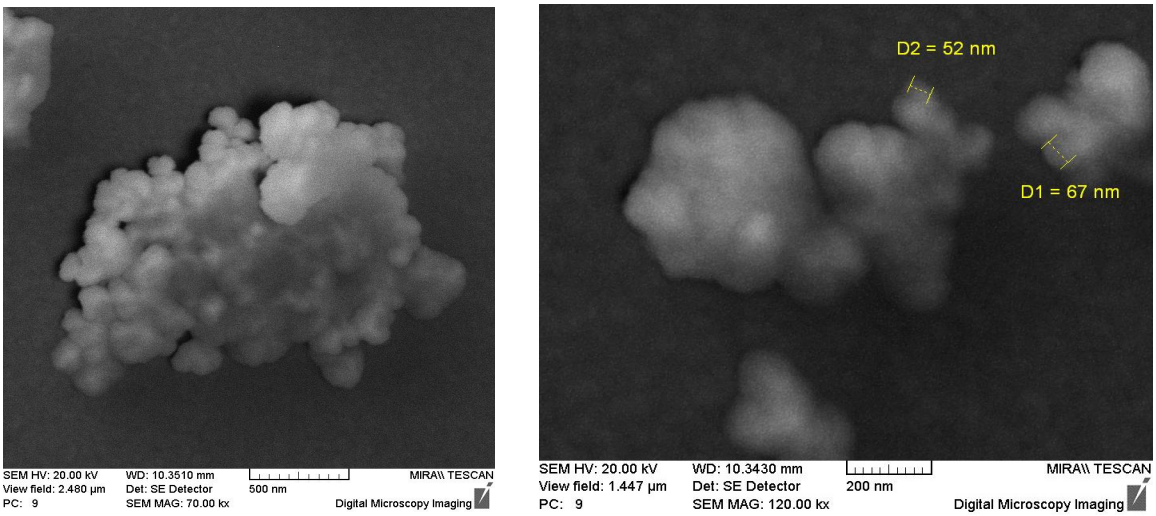

(**a**) (**b**)

Figure 8. SEM images of purified silicon powders obtained from a mixtures with molar ratio $Mg:SiO_2$ = 2:1 (**a**) and 2.5:1 (**b**).

3.2. Study of the Mechanochemical Reduction of Silica by Magnesium

The effects of mechanical treatment duration (in the range from 1 to 8 min at a load value of 60 *g*) and the component ratios in the Mg–SiO_2 system on the reduction of silica with magnesium were studied by XRD analysis. After mechanical activation for 1 min of the sample of stoichiometry composition ($Mg:SiO_2$ = 2:1) the reflections of the initial magnesium, magnesium oxide, silicon, silicide, and magnesium orthosilicate can be identified in the XRD patterns (Figure 9a, curve 1). An increase in activation duration to 2–4 min (Figure 9a, curves 2 and 3) leads to a decrease in the intensity and broadening of the reflexes of all these phases. When the activation time is increased to 8 min, widened reflexes of silicon and magnesium oxide as well as reflexes of magnesium silicide of low intensity are identified (Figure 9a, curve 4).

Investigation of the effect of activation duration (at a load of 60 g and component ratio of $Mg:SiO_2$ = 2.5:1) showed that magnesium reflexes are mainly identified in the X-ray diffraction pattern of the sample after the activation for 1 min (Figure 9b, curve 1). After 2 min activation (Figure 9b, curve 2), intensive reflections of silicon and magnesium oxide together with low intensive peaks of silicide and magnesium orthosilicate appear in the X-ray diffraction patterns, while the intensity of magnesium reflections sharply decreases. A further increase in the activation time from 4 to 8 min (Figure 9b, curves 3 and 4) results

in broadening and a decrease in the intensity of reflections of silicon, magnesium oxide, and magnesium.

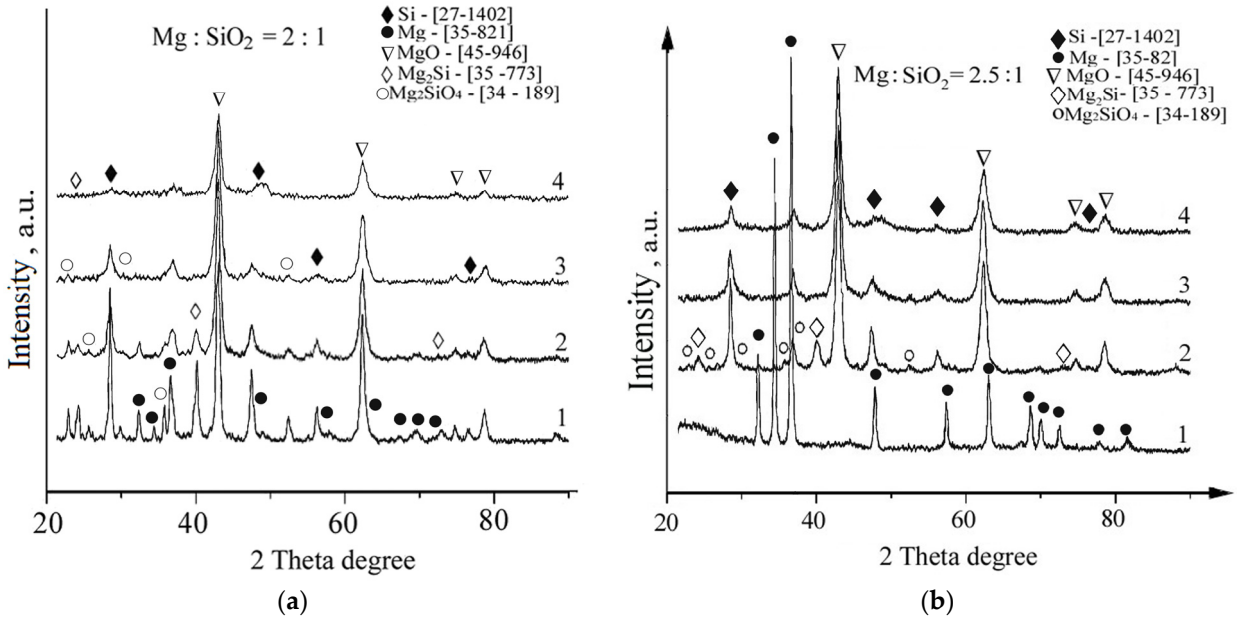

Figure 9. X-ray diffraction patterns of Mg/SiO_2 mechanocomposites (curves 1–4), the composition ratios $Mg:SiO_2$ = 2:1 (**a**); 2.5:1 (**b**); load 60 *g*. Treatment duration: 1 min (1); 2 min (2); 4 min (3); 8 min (4).

To separate silicon from MgO and other byproducts presented in the composition of mechanocomposites, investigations of the treatment of samples with acid solutions were carried out. As in the case of MA SHS, a three-stage acid treatment of the products of mechanochemical reduction of silica with magnesium was carried out.

The XRD data show that after three-stage acid treatment, silicon is purified from the main impurities, such as MgO, Mg_2Si, and Mg_2SiO_4 (Figure 10).

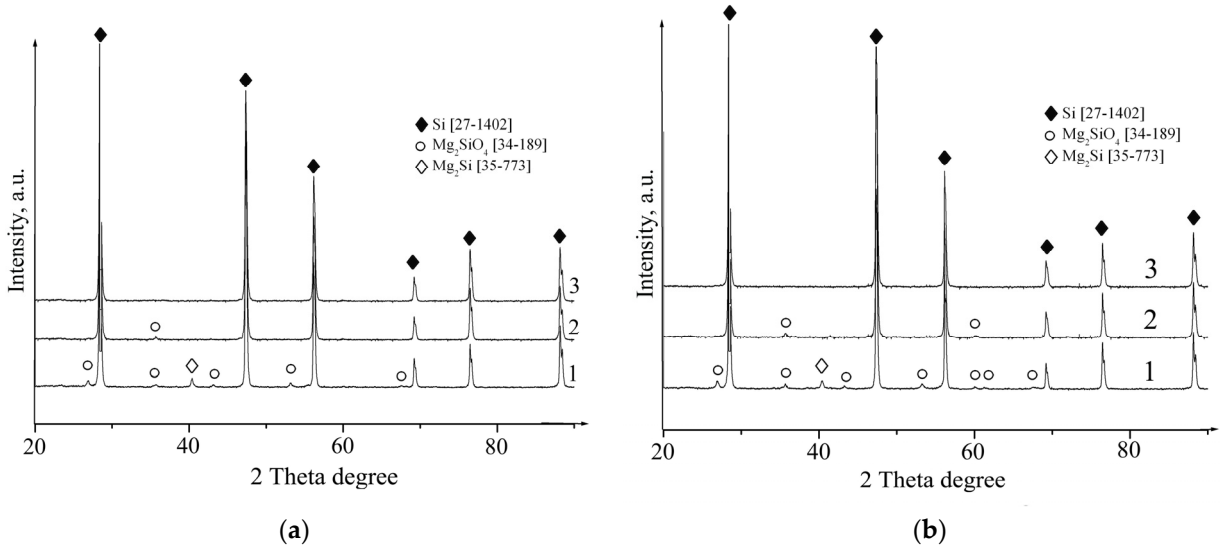

Figure 10. X-ray diffraction patterns of samples of mechanochemical reduction of silica by magnesium: after the first stage of acid treatment (2 M HCl) (1); after the second stage of acid treatment (20% H_3CCOOH, 2 M HCl) (2); after the third stage of acid treatment (20% H_3CCOOH, 5% HF) (3); the ratio of components in the initial mixtures, $Mg:SiO_2$: 2:1 (**a**) and 2.5:1 (**b**).

The results of SEM analysis of the powder morphology (Figure 11) have shown that after separation from byproducts, silicon powders consist of primary particles with a size of ~30–50 nm, making the larger secondary particles —aggregates with sizes from 1 to 10 μm.

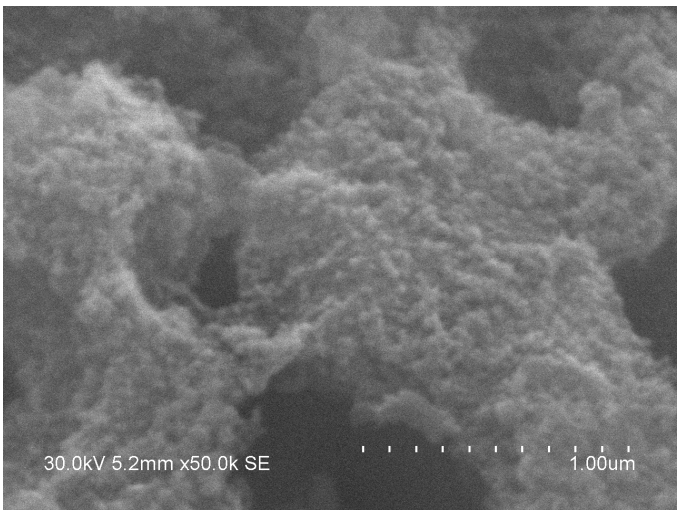

Figure 11. SEM micrograph of purified highly dispersed silicon, produced by the direct mechanochemical reduction of silica by magnesium.

4. Discussion

It is well known that both self-propagating high-temperature synthesis (SHS) reactions [10–12] and mechanically stimulated reactions [38,39] can occur in high-energy systems. The main disadvantage in such systems is extremely high synthesis temperatures, as a result of which the reaction products are melted and coarse. The preliminary joint mechanical activation of initial components allows one to reduce the temperature in the combustion wave and to increase the rate of the overall process [21,36,37,40]. The main reasons for the decrease in the combustion temperature and the increase in the rates of chemical reactions in mechanically activated mixtures are structural changes, namely, the achievement of a high density of interfacial boundaries between initial components, an extremely high contact surface, and a very high concentration of defects due to a large number of atoms on juvenile surfaces and in near-surface layers [41–45]. As a result, the changes in mass transfer and phase formation mechanisms are observed. In the case of composite formation with several levels of heterogeneity, the rate of chemical reactions in the region of interfacial boundaries with nanocomposite structure is much higher compared to the rate of reactions with a micron scale of heterogeneity. These structural changes which occur as a result of mechanical activation contribute to solid-phase reactions in mechanically activated mixtures. A change in the chemical routes in these mixtures may include direct synthesis of the target phase without the formation of intermediates formed in non-activated systems, as well as a change in the type and sequence of reactions instead of those occurring during self-propagating high-temperature synthesis without prior mechanical activation. Thus, the finely dispersed composite particles formed at the stage of mechanical activation contribute to a heterogeneous crystallization in combustion wave and prevent the growth of product grains behind its front.

Our previous studies for the $4Al–3SiO_2$ high-energy system revealed the effect of the size of SiO_2 nanoparticle aggregates on the starting temperature of chemical interaction and phase formation processes in SHS. It was found that, despite the nanosize of the initial silica powder, preheating is necessary to initiate the reaction in the non-activated reaction mixture of $4Al–3SiO_2$. The formation of Al/SiO_2 composite particles during the MA process allows initiating the combustion at room temperature. In this case, the phase composition of MA SHS product depends on the degree of dispersion of SiO_2 inclusions in the aluminum

matrix. The presence of relatively large (micrometric and submicron) aggregates of SiO_2 nanoscale particles leads to the interaction of aluminum oxide formed at the initial stage of SHS with silica to form mullite. When SiO_2 is finely dispersed in aluminum, forming aggregates with dimensions of about 55 nm, the almost instantaneous (the life time of the liquid phase is ≈1 s) one-stage chemical reaction is observed which leads to the formation of Si and α-Al_2O_3.

A significant decrease of the starting temperature for the reaction and an increase of the reaction rate can ensure the realization of mechanostimulated reactions in the activator, as, for example, in the Fe_2O_3-Al [46], Fe_2O_3-Zr [47], and CuO-Zr [48] systems. In this work, a comparative study of MA SHS and MSR in the SiO_2-Mg system was carried out.

The prospects to obtain silicon in the interaction of silica with magnesium depend primarily on the thermodynamic possibility of the reaction, as shown in [49–51].

The reactions that can occur in the Mg-SiO_2 system are presented in Table 2 [52].

Table 2. The thermodynamic parameters for the reactions of silica with magnesium [52].

No.	The Reactions	T = 25 °C		T = 627 °C	
		ΔH, kJ/mol	**ΔG, kJ/mol**	**ΔH, kJ/mol**	**ΔG, kJ/mol**
1	$2Mg + SiO_2 \rightarrow Si + 2MgO$	−292.8	−279	−292.6	−259
2	$2Mg + 3SiO_2 \rightarrow 2MgSiO_3 + Si$	−367.3	−370	−372.2	−346
3	$4Mg + SiO_2 \rightarrow Mg_2Si + 2MgO$	−372.2	−355	−372.2	−330
4	$2Mg + Si \rightarrow Mg_2Si$	−79.5	−77	−80.2	−71
5	$MgO + SiO_2 \rightarrow MgSiO_3$	−37.3	−45	−39.6	−43
6	$2MgO + SiO_2 \rightarrow Mg_2SiO_4$	−63	−72	−63.6	−69

Based on thermodynamic data, it should be expected that reactions 1–3 with the highest formation heats are preferable; the products of reactions 1–3, in addition to Si, are MgO, Mg_2Si, and magnesium silicates. Therefore, there is a task of separating silicon from byproducts. The results of our studies of the combustion process in the Mg-SiO_2 system showed that in a non-activated reaction mixture with a reagent molar ratio Mg:SiO_2 = 2:1, the ignition without preheating of samples is almost impossible. The preheating temperature needed to initiate and realize the SHS process is about 400–550 °C.

The study of the SHS process, where mechanochemically obtained Mg/SiO_2 composites were used as precursors, showed that even a short-term MA (20–60 *g*) allows initiating the combustion process in powder mixtures without preheating. For all compositions studied, very rapid heating was observed due to the course of the magnesium-thermic reaction in the combustion front.

Our studies have shown that the combustion modes during the SHS of mechanically activated mixtures depend on the conditions of the preliminary MA, primarily energy intensity and duration of treatment. The MA of the mixture must be carried out at a rotation speed of 600 rpm for 1–2 min. An increase in the activation time at this rotation speed leads to a decrease in the ignition delay time.

Taking into account the fact that T_C in all cases studied is above the melting point of magnesium (650 °C), but below the melting point of silica (1713 °C) and combustion products (melting points of silicon and magnesium oxide are 1410 °C and 2825 °C, respectively), it is obvious that in the process of SHS using the preliminary formed mechanocomposites, the so-called "combustion with an intermediate molten layer" is realized [22].

The main products of MA SHS are silicon and magnesium oxide; the formation of some amounts of magnesium silicate and silicide is also observed. Since the aim of this work was to obtain nanoscale silicon powder, it was necessary to separate it from byproducts. Hydrochloric acid was used to dissolve magnesium oxide. Some magnesium silicates and silicide were present in the products after leaching with hydrochloric acid. For a more

complete removal of magnesium compounds, the second stage of sample treatment with a mixture of acetic and hydrochloric acids was carried out. The addition of acetic acid made it possible to reduce the adsorption of metal cations on silicon powder. For the final purification of silicon, treatment with a mixture of hydrofluoric and acetic acids was introduced. Three-stage acid treatment [32] is technologically simple to implement, allows one to scale the cleaning process, and provides the production of single-phase nanosize silicon with a particle size of about 50–80 nm and a high degree of silicon purification from Al, Ca, Cd, Cr, Fe, K, Mg, Mn, Ni, and Zn.

Previously obtained results on mechanostimulated reactions have shown that direct mechanochemical reduction of oxides is possible for highly exothermic systems [53–57]. In this paper, the influence of mechanical activation modes on the direct mechanochemical reduction of silica by magnesium was studied. It was shown that the reduction process depends on the energy intensity of the activator, the duration of activation, and the ratio of the components in the mixture. Complete reduction of silica by magnesium can be achieved at a drum rotation speed of $\geq$1000 rpm and activation duration of at least 8 min. The reaction products, as in the case of MA SHS, are silicon, magnesium oxide, and small amounts of Mg_2Si and magnesium silicates. The three-stage acid treatment was carried out to purify Si from the main impurities, such as MgO, Mg_2Si, and Mg_2SiO_4. The silicon powder obtained consists of primary particles with sizes of 30–50 nm, forming secondary particles—aggregates with sizes from 1 to 10 μm.

5. Conclusions

For the first time, direct mechanochemical synthesis of Si via reduction of silica with magnesium has been implemented. The optimal component ratio ($Mg:SiO_2$ = 2.5:1) and the MA parameters (1000 rpm, duration 8 min) have been determined, yielding Si/MgO mechanocomposites without impurity phases of magnesium silicide and magnesium orthosilicate.

SHS has been carried out with preliminary MA of the SiO_2 + 2Mg mixture. MA conditions (600 rpm, duration 40 s) have been determined, providing a decreased combustion temperature (1283–1288 °C) for the formation of SiO_2/Mg composite structures. The optimal ratio of components ($Mg:SiO_2$ = 3:1) for the MA SHS with minimum content of accompanying impurity phases (magnesium silicide and magnesium silicate) has been found.

Three-stage acid treatment of products of both mechanochemical and MA SHS reduction of silica with magnesium allows the obtaining of single-phase nanosize silicon.

The size of powdered silicon particles obtained by the MA SHS is 50–80 nm. In the case of direct mechanochemical synthesis, the size of silicon particles is 30–50 nm.

Thus, the direct mechanochemical reduction of silica with magnesium is preferable compared to mechanically activated, self-propagating high-temperature synthesis, since the process is carried out in one stage and in a short time (no more than 8 min), the reduced products do not contain the Mg_2Si and Mg_2SiO_4 impurity phases, and purified silicon has smaller particle sizes.

Author Contributions: Conceptualization, N.L. and T.G.; investigation, T.T., T.U., S.V. and E.D.; methodology, N.L. and T.G.; resources, S.V.; data curation, T.T.; writing—original draft preparation, T.G., T.U., S.V. and E.D.; writing—review and editing, N.L., T.G., T.T. and E.D.; visualization, T.T., T.U. and E.D.; validation, S.V. and T.U.; funding acquisition, N.L. All authors have read and agreed to the published version of the manuscript.

Funding: The work was supported by the Ministry of Science and Higher Education of the Russian Federation (Reg. number 121032500062-4).

Institutional Review Board Statement: Not applicable.

Informed Consent Statement: Not applicable.

Data Availability Statement: The box numbers shown in Figures 4, 6, 9a,b and 10a,b for Mg, MgO, Mg_2Si, Mg_2SiO_4, and Si crystal phases from the PDF4+ ICDD database are available at reference [34] [DOI:10.1017/S0885715619000812]. The thermodynamic parameters given in Table 2 for the reactions of silica reduction by magnesium are available at reference [52].

Conflicts of Interest: The authors declare no conflict of interest. The funders had no role in the design of the study; in the collection, analyses, or interpretation of data; in the writing of the manuscript, or in the decision to publish the results.

References

1. McDowell, M.T.; Lee, S.W.; Nix, W.D.; Cui, Y. Understanding the lithiation of silicon and other alloying anodes for lithium-ion batteries. *Adv. Mater.* **2013**, *25*, 4966–4985. [CrossRef]
2. McDowell, M.T.; Ryu, I.; Lee, S.W.; Wang, C.; Nix, W.D.; Cui, Y. Studying the kinetics of crystalline silicon nanoparticle lithiation with in situ transmission electron microscopy. *Adv. Mater.* **2012**, *24*, 6034–6041. [CrossRef]
3. Timmerman, D.; Izeddin, I.; Stallinga, P.; Yassievich, I.N.; Gregorkiewicz, T. Space separated quantum cutting with silicon nanocrystals for photovoltaic applications. *Nat. Photon.* **2008**, *2*, 105–109. [CrossRef]
4. Priolo, F.; Gregorkiewicz, T.; Galli, M.; Krauss, T.F. Silicon nanostructures for photonics and photovoltaics. *Nat. Nanotechnol.* **2014**, *9*, 19–32. [CrossRef]
5. Dai, F.; Zai, J.; Yi, R.; Gordin, M.L.; Sohn, H.; Chen, S.; Wang, D. Bottom-up synthesis of high surface area mesoporous crystalline silicon and evaluation of its hydrogen evolution performance. *Nat. Commun.* **2014**, *5*, 3605. [CrossRef]
6. Mason, B.A.; Groven, L.J.; Son, S.F.; Yetter, R.A. Combustion performance of several nanosilicon-based nanoenergetics. *J. Propul. Power* **2013**, *29*, 1435–1444. [CrossRef]
7. Bux, S.K.; Blair, R.G.; Gogna, P.K.; Lee, H.; Chen, G.; Dresselhaus, M.S.; Kaner, R.B.; Fleurial, J.P. Nanostructured bulk silicon as an effective thermoelectric material. *Adv. Funct. Mater.* **2009**, *19*, 2445–2452. [CrossRef]
8. Stoetzel, J.; Schneider, T.; Mueller, M.M.; Kleebe, H.J.; Wiggers, H.; Schierning, G.; Schmechel, R. Microstructure and thermoelectric properties of Si-WSi_2 nanocomposites. *Acta Mater.* **2017**, *125*, 321–326. [CrossRef]
9. Gribov, B.G.; Zinov'ev, K.V. Preparation of high-purity silicon for solar cells. *Inorg. Mater.* **2003**, *39*, 653–662. [CrossRef]
10. Merzhanov, A. Self-propagating high-temperature synthesis: Twenty years of search and findings. In *Combustion and Plasma Synthesis of High-Temperature Materials*; Munir, Z., Holt, J., Eds.; VCH: New York, NY, USA, 1990; pp. 1–53.
11. Merzhanov, A. *Combustion and Synthesis of Materials*; ISMAN Publ.: Chernogolovka, Russia, 1998; 511p.
12. Itin, V.; Naiborodenko, Y. *High-Temperature Synthesis of Intermetallic Compounds*; TSU Publ.: Tomsk, Russia, 1989; 218p.
13. Zakaryan, M.K.; Aydinyan, S.V.; Kharatyan, S.L. Preparation of Fine-grained Silicon from Serpentine Mineral by Magnesiothermic Reduction of Silica in the Presence of Reaction Products as Diluents. *Silicon* **2017**, *9*, 841–846. [CrossRef]
14. Merzhanov, A.; Mukasyan, A. *Combustion of Solid Flame*; Tonus Press: Moscow, Russia, 2007; 336p.
15. Moore, J.J.; Feng, H.J. Combustion Synthesis of Advanced Materials: Part I. Reaction Parameters. *Prog. Mater. Sci.* **1995**, *39*, 243–273. [CrossRef]
16. Varma, A.; Rogachev, A.S.; Mukasyan, A.S.; Hwang, S. Combustion synthesis of advanced materials: Principles and applications. *Adv. Chem. Eng.* **1998**, *24*, 79–226.
17. Rogachev, A.S.; Mukasyan, A.S. *Combustion for Material Synthesis*; CRC Press: Boca Raton, FL, USA, 2014; 424p. [CrossRef]
18. Talako, T. Powders Obtained by the Method of Mechanically Activated Self-Propagating High-Temperature Synthesis for Heat-Resistant, Wear-Resistant and Radio-Absorbing Gas-Thermal Coatings. Ph.D. Thesis, State Scientific and Production Association of Powder Metallurgy, Minsk, Belarus, 2015.
19. Haouli, S.; Boudebane, S.; Slipper, I.J.; Lemboub, S.; Gębara, P.; Mezrag, S. Combustion synthesis of silicon by magnesiothermic reduction. *Phosphorus Sulfur Silicon Relat. Elem.* **2018**, *193*, 280–287. [CrossRef]
20. Zulumyan, N.H.; Isahakyan, A.R.; Hovhannisyan, Z.H.; Torosyan, A.R. The influence of mechanical activation on the process of thermal reduction of silica by magnesium powder. In *Magnesium Technology*; Luo, A., Neelameggham, N., Beals, R., Eds.; The Minerals, Metals & Materials Society (TMS): Pittsburgh, PA, USA, 2006; pp. 351–354.
21. Grigorieva, T.; Korchagin, M.; Lyakhov, N. Combination of SHS and mechanochemical synthesis for nanopowder technologies. *KONA Powder Part. J.* **2002**, *20*, 144–158. [CrossRef]
22. Korchagin, M. Experimental Investigation of the Mechanism of Interaction of Reagents of Self-Propagating High-Temperature Synthesis and Development of Scientific Foundations for the Production of Nanocomposite Materials with a Ceramic-Hardened Phase. Ph.D. Thesis, Altai Polzunov State University, Barnaul, Russia, 2007.
23. Lyakhov, N.; Talako, T.; Grigoreva, T. *Influence of Mechanical Activation on Processes of Phase and Structure Formation by Self-Propagating High-Temperature Synthesis*; Parallel: Novosibirsk, Russia, 2008; 168p.
24. Baláž, P. *Mechanochemistry in Nanoscience and Minerals Engineering*; Springer: Berlin/Heidelberg, Germany, 2008; 413p.
25. McCormick, P.G. Application of mechanical alloying to chemical refining. *Mater. Trans. JIM* **1995**, *36*, 161–169. [CrossRef]
26. Schaffer, G.B.; McCormick, P.G. Displacement reactions during mechanical alloying. *Metall. Trans. A* **1990**, *21*, 2789–2794. [CrossRef]

27. Matteazzi, P.; LeCaër, G. Synthesis of nanocrystalline alumina-metal composites by room-temperature ball-milling of metal oxides and aluminium. *J. Am. Ceram. Soc.* **1992**, *75*, 2749–2755. [CrossRef]
28. Yang, H.; McCormick, P.G. Mechanochemical reduction of V_2O_5. *J. Solid State Chem.* **1994**, *110*, 136–141. [CrossRef]
29. Mukopadhyay, D.K.; Prisbrey, K.A.; Suryanarayana, C.; Froyes, F.H. Ball-milling, a novel extraction process for production of W from WO_3 using magnesium as reductant. In *Tungsten and Refractory Metals 3*; Bose, A., Dowding, R., Eds.; Metal Powder Industries Federation: New York, NY, USA, 1996; pp. 239–346.
30. El-Eskandarany, M.S.; El-Bahnasawy, H.N.; Ahmed, H.A.; Eissa, N.A. Mechanical solid-state reduction of haematite with magnesium. *J. Alloys Compd.* **2001**, *314*, 286–295. [CrossRef]
31. Grigorieva, T.F.; Sharafutdinov, M.R.; Kaminskii, Y.D.; Vorsina, I.A.; Barinova, A.P.; Lyakhov, N.Z.; Talako, T.L.; Tsibulya, S.V. Ultrafine Si/Al_2O_3 composites obtained by combining methods of mechanical activation and self-propagating high-temperature synthesis. *Combust. Explos. Shock. Waves* **2010**, *46*, 36–40. [CrossRef]
32. Raschman, P.; Fedoroĉková, A. Study of inhibiting effect of acid concentration on the dissolution rate of magnesium oxide during the leaching of dead-burned magnesite. *Hydrometallurgy* **2004**, *71*, 403–412. [CrossRef]
33. Smith, A. *Applied Infrared Spectroscopy*; Wiley: New York, NY, USA, 1979; 332p.
34. Gates-Rector, S.; Blanton, T. *Powder Diffraction File PDF4+ ICDD Release*; Cambridge University Press: Cambridge, MA, USA, 2020. [CrossRef]
35. Shaw, A.P.G. *Thermitic Thermodynamics*; CRC Press: Boca Raton, FL, USA, 2020; 1094p. [CrossRef]
36. Korchagin, M.A.; Grigorieva, T.F.; Bokhonov, B.B.; Sharafutdinov, M.R.; Barinova, A.P.; Lyakhov, N.Z. Solid-State Combustion in Mechanically Activated SHS Systems. I. Effect of Activation Time on Process Parameters and Combustion Product Composition. *Combust. Explos. Shock. Waves* **2003**, *39*, 43–50. [CrossRef]
37. Korchagin, M.A.; Grigorieva, T.F.; Bokhonov, B.B.; Sharafutdinov, M.R.; Barinova, A.P.; Lyakhov, N.Z. Solid-State Combustion in Mechanically Activated SHS Systems. II. Effect of Mechanical Activation Conditions on Process Parameters and Combustion Product Composition. *Combust. Explos. Shock. Waves* **2003**, *39*, 51–58. [CrossRef]
38. Takacs, L. Reduction of magnetite by aluminum: A displacement reaction induced by mechanical alloying. *Mater. Lett.* **1992**, *13*, 119–124. [CrossRef]
39. Schaffer, G.B.; McCormic, P.G. Combustion synthesis by mechanical alloying. *Scr. Met.* **1989**, *23*, 835–838. [CrossRef]
40. Korchagin, M.A.; Grigorieva, T.F.; Barinova, A.P.; Lyakhov, N.Z. The effect of mechanical treatment on the rate and limits of combustion in SHS processes. *Intern. J. SHS* **2000**, *9*, 307–320.
41. Benjamin, J.S. Mechanical alloying. *Sci. Am.* **1976**, *234*, 40–58. [CrossRef]
42. Gilman, P.S.; Benjamin, J.S. Mechanical alloying. *Ann. Rev. Mater. Sci.* **1983**, *13*, 279–300. [CrossRef]
43. Koch, C.C. Materials synthesis by mechanical alloying. *Ann. Rev. Mater. Sci.* **1989**, *19*, 121–143. [CrossRef]
44. Eckert, J.; Holzer, J.C.; Krill, C.E.; Johnson, W.L. Structural and Thermodynamic Properties of Nanocrystalline fcc Metals Prepared by Mechanical Attrition. *J. Mat. Res.* **1992**, *7*, 1751–1761. [CrossRef]
45. Cabouro, G.; Chevalier, S.; Gaffet, E.; Vrel, D.; Boudet, N.; Bernard, F. In situ synchrotron investigation of $MoSi_2$ formation mechanisms during current-activated SHS sintering. *Acta Mater.* **2007**, *55*, 6051–6063. [CrossRef]
46. Grigoreva, T.F.; Kiseleva, T.Y.; Petrova, S.A.; Talako, T.L.; Vosmerikov, S.V.; Udalova, T.A.; Devyatkina, E.T.; Novakova, A.A.; Lyakhov, N.Z. Mechanochemically Stimulated Reactions of the Reduction of Iron Oxide with Aluminum. *Phys. Met. Metallogr.* **2021**, *122*, 572–578. [CrossRef]
47. Kiseleva, T.; Letsko, A.; Talako, T.; Kovaleva, S.; Grigoreva, T.; Novakova, A.; Lyakhov, N. Mossbauer spectroscopy study of Fe/ZrO_2 nanocomposites formation by MA SHS technology. *Hyperfine Interact.* **2018**, *239*, 14. [CrossRef]
48. Grigoreva, T.F.; Šepelák, V.; Vorsina, I.A.; Letsko, A.I.; Talako, T.L.; Ilyushchenko, A.F.; Lyakhov, N.Z. Cu/ZrO_2 composites prepared by self-propagating high-temperature processing of the mechanically pre-activated system. *Powder Metall. Prog.* **2011**, *11*, 284–289.
49. Lidin, R.; Molochko, V.; Andreeva, L. *Khimicheskie Svoistva Neorganicheskikh Veshchestv*, 4th ed.; Kolos: Moscow, Russia, 2003; 480p.
50. Veryatin, U.; Mashirev, V.; Ryabtsev, N.; Tarasov, V. *Termodinamicheskie Svoistva Neorganicheskikh Veshchestv*; Atomizdat: Moscow, Russia, 1965; 461p.
51. *Spravochnik Khimika*, 2nd ed.; Khimiya: Moscow-Leningrad, Russia, 1966; Volume 1, pp. 802–803.
52. Kiselev, A.D. Processes for the Production of Silicon with a Low Content of Impurities Using Magnetothermic Reduction of Silicon Dioxide in Tight Drop Apparatuses. Ph.D. Thesis, National Research Tomsk Polytechnic University, Tomsk, Russia, 2014.
53. Pavlov, E.A.; Udalova, T.A.; Grigoreva, T.F.; Vosmerikov, S.V.; Vorsina, I.A.; Devyatkina, E.T.; Lyakhov, N.Z. Preparing Ultradisperse Copper Powder via the Mechanochemical Reduction of Copper Oxides by Magnesium. *Bull. Russ. Acad. Sci. Phys.* **2018**, *82*, 574–577. [CrossRef]
54. Udalova, T.A.; Vosmerikov, S.V.; Grigoreva, T.F.; Devyatkina, E.T.; Lyakhov, N.Z. Fine Tungsten from W/MgO Mechanocomposite Obtained by the Reduction of Tungsten (VI) Oxide by Magnesium. *Chem. Sustain. Dev.* **2019**, *27*, 304–309. [CrossRef]
55. Udalova, T.A.; Grigoreva, T.F.; Devyatkina, E.T.; Vosmerikov, S.V.; Lyakhov, N.Z. Mechanochemical Reduction of GeO_2 with Magnesium. *Chem. Sustain. Dev.* **2018**, *26*, 537–542. [CrossRef]

56. Lyakhov, N.Z.; Udalova, T.A.; Grigoreva, T.F. Mechanochemical way of obtaining highly dispersed metal powders. In Proceedings of the Nano-2020, 7th All-Russian Conference on Nanomaterials (NANO-2020), Moscow, Russia, 18–22 May 2020; IMET RAS Publish: Moscow, Russia, 2020; pp. 10–11.
57. Udalova, T.A.; Vosmerikov, S.V.; Grigoreva, T.F.; Devyatkina, E.T.; Lyakhov, N.Z. Mechanochemical synthesis of highly dispersed tungsten and molybdenum. In Proceedings of the Thermodynamics and Materials Science, Abstracts of the 13th Symposium with International Participation Thermodynamics and Materials Science, Novosibirsk, Russia, 26–30 October 2020; Gelfond, N.V., Ed.; NIIC SB RAS Publish: Novosibirsk, Russia, 2020; p. 54.